



Soil phosphorus fractions dynamics along a 22-ka chronosequence of landslides, western Sichuan, China

Junbo He^{a,b}, Yanhong Wu^{a,*}, He Zhu^a, Jun Zhou^a, Chaoyi Luo^{a,b}, Haijian Bing^a

^a Institute of Mountain Hazards and Environment, Chinese Academy of Sciences, Chengdu 610299, China

^b University of Chinese Academy of Sciences, Beijing 100049, China

ARTICLE INFO

Keywords:

Landslides chronosequence
Pedogenesis
Soil phosphorus fractions
Bioavailable phosphorus

ABSTRACT

Landslides significant influence on bedrock weathering, pedogenesis, and ecological succession, thereby playing a pivotal role in driving biogeochemical cycles. Landslide chronosequences have traditionally served as invaluable study systems for investigating vegetation succession and exploring soil development and nutrient dynamics. In this study, we analyzed soil phosphorus fractions across a 22,000-year landslide chronosequence. Our investigation examined the impact of environmental factors on these fractions and elucidated the supply of bioavailable phosphorus. Our findings revealed a decline in the concentration of all phosphorus fractions with soil age. Notably, even at an age exceeding 22,000 years, primary mineral phosphorus constituted 23 % of the total phosphorus pool at the later stages of soil development, while organic phosphorus accounted for a mere 7 %. This discrepancy can be attributed to frequent landslides replenishing phosphorus stocks. These findings indicate that the Walker and Syers model may not adequately anticipate alterations in soil phosphorus fractions under geologically unstable landscapes. Environmental factors had limited impact on primary mineral phosphorus concentrations. Yet, they significantly influenced occluded and nonoccluded phosphorus. Changes in organic phosphorus concentrations cannot be fully explained by the examined environmental factors, as organic phosphorus in the soil primarily originates from plant litter decomposition. The sources of bioavailable phosphorus in the investigated region were elucidated using structural equation modeling. The bioavailable phosphorus in the study area is mainly derived from nonoccluded phosphorus rather than organic phosphorus. This observation can be attributed to the distinct landform conditions, which sustain elevated levels of primary mineral phosphorus during soil development. Consequently, the continuous availability of nonoccluded phosphorus ensures a reliable supply of bioavailable phosphorus. In conclusion, the landslide chronosequence serves as a vital example of long-term ecosystem development under unstable landforms. Its refinement of the Walker and Syers model under unstable landscapes.

1. Introduction

Landslides, as the predominant erosional mechanism in mountainous regions worldwide, exert a profound influence on landscape evolution by counteracting active uplift processes and shaping mountain topography (Parker et al., 2011; Geertsema et al., 2006). These rapid geohazard events involve the downward movement of bedrock, soil, and debris along slopes, occurring when destabilizing forces surpass stabilizing forces (Cruden and Varnes, 1996; Cruden, 1991). Triggers for landslides encompass seismic activity, intense precipitation, ice thawing, and human activities (Walker et al., 2009). Despite advancements in

technology and research, landslides remain largely unpredictable, posing a persistent threat to human populations in mountainous areas and leading to annual fatalities (Petley, 2012). Simultaneously, landslides play a crucial role in biogeochemical cycles by facilitating the transport of substantial amounts of terrestrial organic carbon and sediments to the ocean through river systems (Hilton et al., 2008; Korup, 2004; Tate et al., 2000). During landslide events, nutrients present in rocks and soils undergo physical and chemical processes, releasing and transporting them into water bodies. Essential nutrients such as nitrogen, phosphorus, potassium, and various others exert substantial influence on the nutrient cycling dynamics and productivity of aquatic

* Corresponding author.

E-mail addresses: hejunbo@imde.ac.cn (J. He), yhwu@imde.ac.cn (Y. Wu), zhuhe@imde.ac.cn (H. Zhu), zhoujun@imde.ac.cn (J. Zhou), luochaoyi@imde.ac.cn (C. Luo), hjbing@imde.ac.cn (H. Bing).

<https://doi.org/10.1016/j.catena.2023.107674>

Received 31 August 2023; Received in revised form 19 October 2023; Accepted 3 November 2023

0341-8162/© 2023 Published by Elsevier B.V.

ecosystems. The global occurrence of landslides is currently on the rise due to global warming (Evans and Clague, 1994), yet the implications of the changing feedback mechanisms between landslides, climate, and the biosphere remain uncertain. Following a landslide event, the deposited material primarily consists of bedrock, along with soil and remnants of vegetation. Throughout the process of succession, this material undergoes a series of physicochemical transformations (Cui et al., 2022). These transformations entail the liberation of primary mineral phosphorus via weathering, the accretion of organic carbon and reactive nitrogen facilitated by biological activities, and modifications in slope stability. Collectively, these processes engender the formation of a nascent soil mantle, ultimately fostering the colonization of vegetation (Bogaart and Zee, 2010). Consequently, landslides not only represent significant disturbance events but also create unique ecological niches and foster biodiversity.

Soil chronosequences derived from landslides offer a valuable approach for studying soil development and nutrient dynamics in mountainous regions worldwide, thereby enhancing our understanding of the intricate interactions between landslides, climate, and the biosphere (Blonska et al., 2018; Hemingway et al., 2018; Schulz et al., 2013; Hilton et al., 2011; Schmidt et al., 2008). Establishing a landslide soil chronosequence poses another significant challenge, namely, the requirement for consistent lithological compositions across the landslides. In other words, it is crucial to ensure the uniformity of the parent material from which the soils are formed (Walker et al., 2010). Consequently, landslide soil chronosequences are primarily examined by selecting soils with similar parent materials within the same geological context. The majority of landslide chronosequences span relatively short time scales, dating back a few centuries, there have been reports of chronosequences dating as far back as 13,000 years (Vindusková et al., 2019). However, the long-term dynamic of phosphorus (P) on landslide chronosequences are remains largely understudied, especially for some eco-environmental fragile and climatically sensitive areas. Phosphorus is an indispensable nutrient for plants and plays a crucial role in maintaining the stability of terrestrial ecosystems, alongside carbon (C) and nitrogen (N) (Westheimer, 1987; Watanabe and Ortega, 2011; Adil et al., 2003). Within the ecosystem, the total P (Pt) pool is typically substantial; however, only the soluble orthophosphate, known as bioavailable P (P-bio), can be directly assimilated by organisms (Tiessen and Moir, 1993). In general, the concentrations of P-bio exhibit a rapid increase during the initial decades of soil development. This phenomenon can be attributed to the ongoing release of primary mineral P from rock sources during the early stages of soil formation, facilitating the accumulation of P-bio. However, as soil development progresses, soil P-bio decreases rapidly, there are two key factors at play. Firstly, all phosphorus fractions within the soil experience a significant decline, primarily driven by surface runoff processes. Secondly, the decrease in P-bio becomes more pronounced because of its utilization by plants and microorganisms (Wu et al., 2015). Therefore, at the later stages of soil development, the bioavailability of P often acts as a limiting factor for ecosystem productivity and vegetation succession (Vitousek et al., 2010). In soils characterized by stable landforms, P limitations can become severe enough to impede plant biomass, productivity, and other essential ecosystem processes, referred to as 'ecosystem retrogression' (Wardle et al., 2004). Furthermore, these limitations can exert a significant effect on the distribution and diversity of plant and microbial communities (Wilkinson, 2008).

The western Sichuan region, located on the eastern edge of the Tibetan Plateau, is renowned for its eco-environmental fragility and climatic sensitivity, making it a significant area of interest for ecological research in China (Wang et al., 2021). Serving as a crucial ecological barrier and water conservation zone for the upper reaches of the Yangtze River and Yellow River, this region holds immense ecological value (Lu et al., 2021). With its distinctive physical geography and geological attributes, the western Sichuan region stands out as one of the most vulnerable areas in China when it comes to the occurrence of landslides

and debris flows (Lu et al., 2021). Consequently, it presents an ideal opportunity to study a landslide chronosequence. To address this research gap, we selected 14 landslides and employed long-term geological dating methods to establish a comprehensive 22,000-year landslide chronosequence on the upper reach of the Minjiang River, western China, as discussed in a separate work (submitted to the Journal of Mountain Science; He et al., 2023). The investigation revealed a consistent and gradual alteration of weathering indices in response to soil development across 14 landslide sites, without any notable anomalous variations along the soil chronosequence. This finding provides evidence supporting the reliability of the landslide chronosequence.

In this study, we conducted a comprehensive analysis of soil P fractions along a landslide chronosequence spanning approximately 22,000 years of pedogenesis in western Sichuan, China. The primary objective of this research was to quantify the temporal changes in soil P fractions, investigate the effect of environmental factors on these fractions, and elucidated the supply of P-bio. We hypothesized that the long-term dynamics of soil P fractions in the study area would deviate from the predictions of the Walker and Syers (1976) model, primarily due to the specific landform characteristics of the study area. Additionally, it was hypothesized that the environmental factors within the study area would exert a substantial influence on the alterations observed in soil phosphorus fractions. Furthermore, we envisage that throughout the protracted process of soil development, organic phosphorus (Po) will emerge as a principal contributor to the P-bio.

2. Materials and methods

2.1. Study area and soil sampling

The study area, located in western Sichuan, China, encompasses the upper reach of the Minjiang River (103°32'-104°15'E, 30°45'-30°09'N). The region's climate is primarily influenced by the Westerlies and the Tibetan Plateau monsoon, as reported by Chen et al. (2022). The annual temperature ranges from 5 to 22 °C, while the mean annual precipitation is approximately 805–962 mm, with most precipitation occurring during the summer months (Fang, 1994; Fang et al., 2003) (Fig. 1). The estimated annual evaporation rates in the study area range from 1725 to 2570 mm. The region exhibits a mountainous topography, with elevations varying from 762 to 5,963 m and a mean elevation of approximately 3,500 m (Fig. 1). Since the Cenozoic, the Tibetan Plateau has been an active geological region uplifted by the collision between the Eurasian and Indian plates (Zhong et al., 2022; Han et al., 2015). As a result, the study area has complex geological conditions, frequent geological hazards, and a fragile ecological environment (Lu et al., 2021). Soil samples were collected from landslides that had been entirely reset by the landslide event. To avoid human disturbance, we selected sites that were not located on large, intact landslide blocks, and we preferred lower central parts of the landslides (Table 1).

All sampling sites were in flat and similar topographic positions, thereby ensuring uniformity in the composition of the lithological. At each site, we established a representative 10 × 10 m plot and collected soil samples from the surface horizon (0–10 cm). Each soil sample was composed of three random sub-samples. The litter layers were removed when collecting the surface horizon soil. In addition, an undisturbed core sample was collected using steel cylinders (100 cm³) to measure soil bulk density. Prior to analysis, plant roots and rock gravels were removed, and the fresh soil sample was passed through a 2 mm sieve and divided into two sub-samples. One sub-sample was kept at 4 °C for the analysis of soil C, N, and P, while the other was air-dried for the analysis of soil physical and chemical properties (He et al., 2023).

2.2. Physical and chemical analysis

The pH values of soil samples were determined using a pH monitor (HACH HQ30D, USA) with a soil-to-water ratio of 1:2.5 (w/v). The

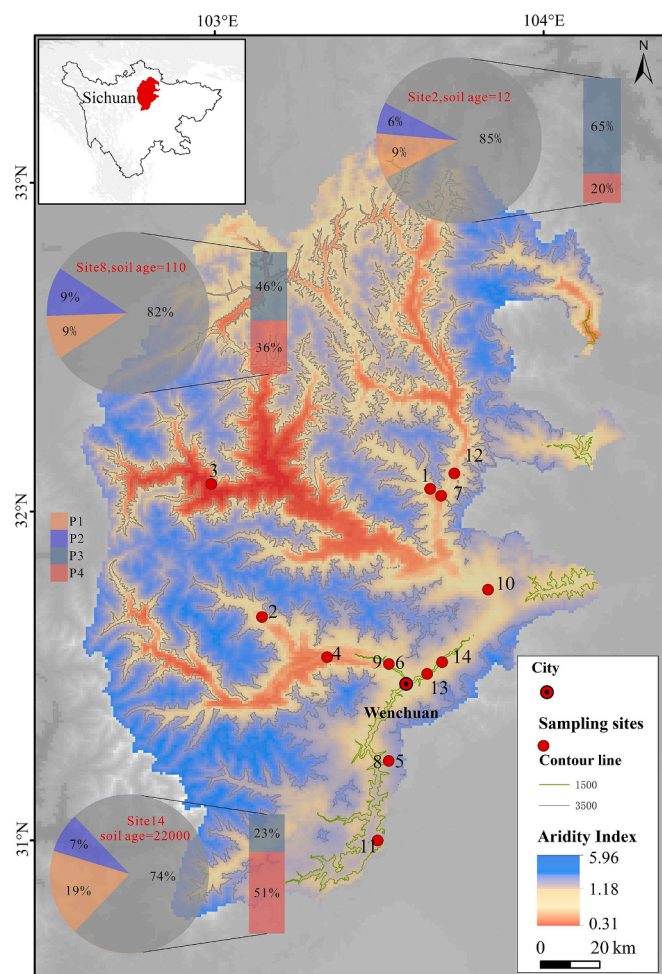


Fig. 1. Location of the study area, the upper reach of Minjiang River, Western Sichuan, China. P1: nonoccluded phosphorus (sum of $\text{NaCHO}_3\text{-Pi}$, NaOH-Pi); P2: organic phosphorus (sum of $\text{NaHCO}_3\text{-Po}$ and NaOH-Po); P3: primary mineral phosphorus (HCl-P); P4: occluded phosphorus (Residual-P).

concentrations of major elements (Al, Ca, Fe, K, Mg, Mn, Na, and Ti) were analyzed using an American Leeman Labs Profile inductively coupled plasma atomic emission spectrometer (ICP-AES). The soil C and N concentrations were measured using an Elementar Vario ISOTOPE cube (EA-IRMS, Germany). Soil Pt was measured by digestion with sulphuric-perchloric acid at 360 °C, and the extraction solution was diluted to 100 mL volume. The concentrations of soil Pt were measured

Table 1
List of studied landslides.

| ID | Full name | Age (y) ^a | Location | | Altitude (m) | Age published first in |
|----|-----------|----------------------|-------------|------------|--------------|------------------------|
| | | | Longitude E | Latitude N | | |
| 1 | Xinmo | 5 | 103.65514 | 32.068647 | 2250 | Xu et al., 2017 |
| 2 | Tasi | 12 | 103.143368 | 31.679613 | 2100 | Gan et al., 2015 |
| 3 | Luhua | 15 | 102.989604 | 32.083414 | 2350 | Wang et al., 2007 |
| 4 | Jianshan | 42 | 103.340866 | 31.557639 | 1900 | Xie et al., 2004 |
| 5 | Fotangba2 | 58 | 103.528527 | 31.241238 | 1670 | Xie et al., 2004 |
| 6 | Chayuan2 | 74 | 103.529226 | 31.536676 | 1350 | Wang et al., 2007 |
| 7 | Diexi | 89 | 103.688266 | 32.047831 | 2325 | Nie et al., 2004 |
| 8 | Fotangba1 | 110 | 103.528527 | 31.241238 | 1670 | Xie et al., 2004 |
| 9 | Chayuan1 | 134 | 103.529226 | 31.536676 | 1350 | Wang et al., 2007 |
| 10 | Huahong | 300 | 103.831129 | 31.762311 | 1810 | Chai et al., 1995 |
| 11 | Shimenkan | 1000 | 103.494763 | 30.999352 | 1510 | Chai et al., 1995 |
| 12 | Qiangyang | 5500 | 103.728402 | 32.115634 | 2180 | An et al., 2008 |
| 13 | Koushan | 14,000 | 103.645949 | 31.506586 | 1500 | Chai et al., 1995 |
| 14 | Wenzhen | 22,000 | 103.69139 | 31.542233 | 1825 | Wang et al., 2007 |

after acid digestion (HNO_3 , HClO_4) by the molybdenum blue method using spectrophotometry at 889 nm. To determine the degree of soil weathering, the chemical index of alteration (CIA) was calculated using a combination of concentrated HNO_3 , HF, and HClO_4 (volume ratios of 3:1:1) in the high-pressure digestion tank. CIA was calculated based on the following formula (1) (Nesbitt and Young, 1982):

$$CIA = \left[\frac{\text{Al}_2\text{O}_3}{\text{Al}_2\text{O}_3 + \text{CaO}^* + \text{Na}_2\text{O} + \text{K}_2\text{O}} \right] \times 100\% \quad (1)$$

where CaO is calculated based on the molar ratio of $\text{CaO}/\text{Na}_2\text{O}$ in soil samples. If the ratio is greater than 1, the content of Na_2O is used to replace the CaO content; otherwise, CaO is equivalent to the measured CaO (McLennan, 1993).

2.3. Soil microbial analyses

To investigate the impact of microbial properties on the regulation of various soil P pools, we analyzed a range of microbial parameters, including microbial biomass C, N, P, and soil phosphatase activity. Specifically, microbial biomass C, N, and P were determined using the chloroform fumigation-extraction method as described by Brookes et al. (1982), while soil phosphatase activity was also measured. For a more detailed description of the methods used, please refer to Chen et al. (2016). To calculate soil microbial biomass P density (MPD, kg P m^{-2}), we used Eq. (3) as described by Tian et al. (2006).

$$MPD = T \times BD \times P_{mic} \times \frac{1 - C}{100} \quad (2)$$

where T is soil thickness (10 cm), BD is bulk density (g cm^{-3}), P_{mic} is the content of soil microbial biomass P (mg kg^{-1}), C is rock content (>2mm).

Soil potential phosphatase activity was determined following the method of German et al. (2011). Briefly, 2 g of fresh soil was extracted with 90 mL of 50 mmol/L acetate buffer. Subsequently, a soil suspension (200 μL) and 4-MUB-phosphate (50 μL , 200 $\mu\text{mol/L}$) were added to 96-well black microplates. After incubation at 15 °C for 3.5 h, the fluorescence was measured using a modular multimode microplate reader (Synergy H1MF, BioTek, USA), with excitation and emission wavelengths of 365 nm and 450 nm, respectively. Standard curves were established for each soil sample using 200 μL of soil suspension and 50 μL of standard solution (4-MUB). Soil phosphatase activity was expressed as nmol activity per gram of dry soil per hour.

2.4. Climate datasets

Meteorological data on mean annual temperature (MAT) and mean annual precipitation (MAP) from western Sichuan were obtained from

the National Meteorological Information Center (<https://data.cma.cn>) for the period of 2010–2022. Spatial datasets of MAT and MAP at a resolution of 10 km × 10 km were created using Kriging interpolation in ArcMap 10.3 (Environmental Systems Research Institute, Inc., Redlands). MAT and MAP values at 14 sampling sites were extracted from the spatial datasets using geographic coordinates. The aridity index (AI), which represents the ratio of precipitation to potential evapotranspiration, was obtained from the CGIAR-CSI Global-Aridity and Global-PET database (<https://www.cgiar-csi.org>; Zorner et al., 2008). Aridity was calculated as 1 minus AI (Delgado-Baquerizo et al., 2013).

2.5. Sequential phosphorus fractionation

Soil P fractions were measured using a modified sequential extraction method, following the protocols of Hedley and Stewart (1982) and Tiessen and Moir (1993). Specifically, 1 g of air-dried soil samples were mixed with 30 mL of deionized water and an anion-exchange resin bag, and shaken for 16 h at 25 °C. The resin bag was then removed and placed in a clean 50 mL centrifuge tube with 20 mL of 0.5 M HCl to extract the resin-P after shaking for 12 h. Next, the NaHCO₃-P fraction was extracted by shaking the soil with 30 mL of 0.5 M NaHCO₃ (pH = 8.5) overnight (16 h). Sequential extractions were then performed to extract NaOH-P and dilute HCl-P using 0.5 M NaOH and 1 M HCl, respectively. The concentrated HCl-P fraction was extracted with concentrated HCl in a water bath at 80 °C. Finally, residual P was determined by digesting the soil residue in CHCl₃-HClO₄.

Inorganic phosphorus fractions, including NaHCO₃-Pi, and NaOH-Pi, were directly quantified using the molybdate colorimetry method. Total P fractions (NaHCO₃-Pt and NaOH-Pt) in the extractant were determined after digestion with K₂S₂O₈-H₂SO₄ in an autoclave at 121 °C. Organic P fractions (NaHCO₃-Po and NaOH-Po) were calculated as the difference between the Pt and Pi of each fraction. Hedley P fractions were classified into five categories based on their turnover rates and chemical properties (Hou et al., 2018). Bioavailable phosphorus (P-bio) P were defined as the resin-P. Nonoccluded phosphorus was defined as the sum of NaHCO₃-Pi and NaOH-Pi. Organic P was defined as the sum of NaHCO₃-Po and NaOH-Po. Primary mineral P were defined as the HCl-P. Occluded P were defined as the residual-P. Pt was calculated as the sum of all extracted Hedley P fractions. Additionally, the soil P distribution (SPD) (kg P m⁻²) of each P fraction at each sampling site was calculated using Eq. (2) (Tian et al., 2006).

$$SPD = T \times BD \times P_c \times \frac{1 - C}{100} \quad (3)$$

where T is soil thickness (10 cm), BD is bulk density (g cm⁻³), PC is the content of different P fractions (mg kg⁻¹), C is rock content (>2mm).

2.6. Statistical analyses

Prior to data analysis, all data underwent normality checks and logarithmic transformations were applied where necessary. A regression model utilizing the age of the landslide as the sole predictor was selected as the best fit. To ensure comparability of parameter estimates, all parameter coefficients were normalized using z-score conversion. Statistical analyses were conducted using SPSS 19.0 (IBM SPSS, USA) for independent samples t-tests and Kruskal-Wallis tests, while R version 4.0.5 was used for all other analyses.

3. Results

3.1. Soil physicochemical properties and nutrients

The soil samples analyzed in this study ranged in age from 5 to 22,000 years. The concentrations of soil total C increased with time, reaching maximum values in intermediate-aged soils, and total C

concentrations ranged from 2.67 to 16.19 g/kg (Fig. 2a). The concentrations of soil N exhibited a consistent and pronounced increasing trend (Fig. 2b). These findings align well with previous investigations that have explored the changes in topsoil N concentration during soil pedogenesis (Poeplau et al., 2011; Yang et al., 2016). The rapid accumulation of soil N can be attributed to various processes, including biological N fixation, where symbiotic N-fixing organisms dominate in the early stages of ecosystem development, as well as slower inputs from atmospheric deposition and dispersed sources of biological fixation (Vitousek et al., 2010). In contrast, the concentrations of soil Pt exhibited a negative correlation with soil age during the process of soil development, with a gradual decline of approximately 89 % over the entire time span (Fig. 2c). This observed pattern in soil Pt concentration variation along the chronosequence aligns with the dynamics of soil Pt during soil formation, as elucidated by prior studies (Wu et al., 2015; Wardle et al., 2004; Walker and Syers, 1976; Kouno et al., 1995). The pH of the soils exhibited a decreasing trend with soil age, ranging from 8.53 in the youngest soil (5 years) to 7.11 in the oldest soil (22,000 years) (Fig. 2d). Moreover, the clay content of the soils exhibited an increasing trend with soil age, ranging from 2.06 % to 6.63 % (Fig. 2e). The concentration of soil organic matter (SOM) displayed a distribution ranging from 4.21 to 23.92 g/kg, with a mean value of 12.20 g/kg (Fig. 2f).

3.2. Soil alkaline phosphatase and microbial biomass carbon, nitrogen, and phosphorus

Notable changes were observed in the enzymatic activity of alkaline phosphatase (ALP) as well as the concentrations of soil microbiota carbon, nitrogen, and phosphorus (MBC, MBN, MBP) soil along the landslide chronosequence. Regarding ALP activity, a rapid increase (from 690 to 3734 nmol/h·g) was observed during the initial 5 to 42 years of soil development (Sites 1–4), followed by a subsequent decline (from 3734 to 1221 nmol/h·g) between 42 and 110 years of soil development (Sites 4–8). Eventually, ALP activity reached a stable level (ranging between 690 and 1270 nmol/h·g) during the period spanning 110 to 22000 years (Sites 8–14) (Fig. 3d). The concentrations of MBC and MBN exhibited a rapid increase from 87.75 and 7.65 mg/kg, respectively, to 302.11 and 29.85 mg/kg, respectively, during the period spanning 5 to 89 years of soil development (Sites 1–7). Subsequent to this, the rate of increase in concentrations of MBC and MBN decelerated, leading to average concentrations ranging from 289.51 to 368.53 mg/kg and from 29.85 to 42.26 mg/kg, respectively, across soil ages spanning from 89 to 22,000 years (Sites 7–14) (Fig. 3a, b). The concentration of MBP displayed an ascending trend, rising from 3.68 to 19.58 mg/kg over a span of 5 to 42 years of soil development (Sites 1–4). However, between 42 and 110 years of soil development (Sites 4–8), the concentration of MBP declined from 19.58 to 6.16 mg/kg. For soil ages ranging from 110 to 22000 years (Sites 8–14), the concentration of MBP tended to stabilize, with a mean distribution ranging between 5.72 and 7.30 mg/kg (Fig. 3c).

3.3. Soil phosphorus fractions

Among the P fractions, Resin-P constituted a minor proportion, accounting for less than 5 % (average 2.2 %) of the Pt. However, its concentration increased with soil age from 12.81 to 42.26 mg/kg (representing 1.95–4.73 % of Pt) during the 5 to 42-year soil development period. Interestingly, as the soil continued to develop, the concentrations of Resin-P experienced a rapid decline, reaching 1.01 mg/kg (Fig. 4). NaHCO₃-Pi, another P fraction, exhibited relatively low concentrations compared to other fractions. Its concentrations ranged from 6.63 to 42.93 mg/kg (accounting for 2.03–4.83 % of Pt). Similar to Resin-P, NaHCO₃-Pi displayed a comparable trend. The concentrations of NaHCO₃-Po, representing a smaller fraction of Pt (1.59–4.06 % of Pt), declined with soil age, ranging from 1.39 to 39.18 mg/kg (Fig. 4). Moving on to NaOH-Pi and NaOH-Po, these fractions accounted for a

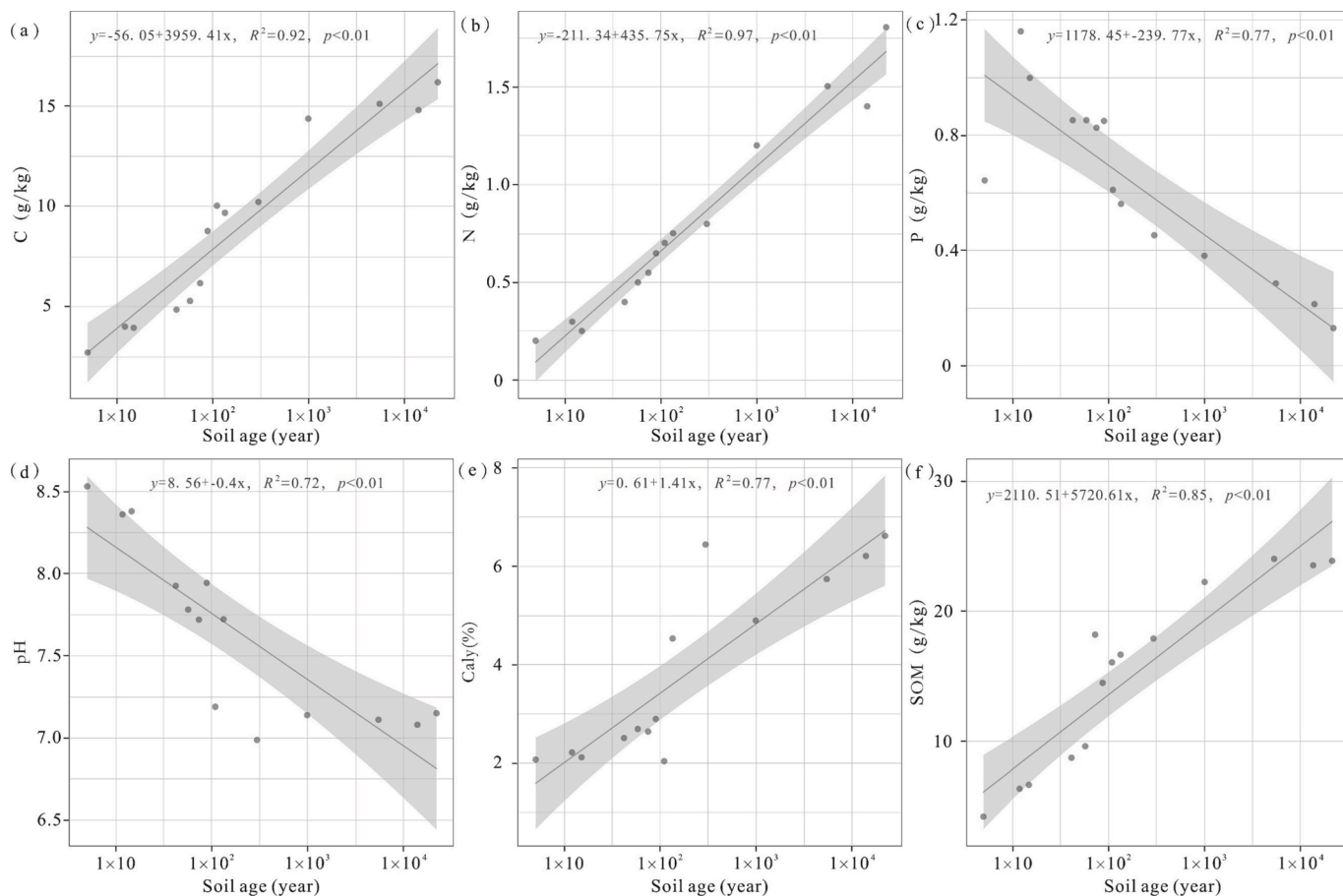


Fig. 2. Changes in soil characteristics with soil age.

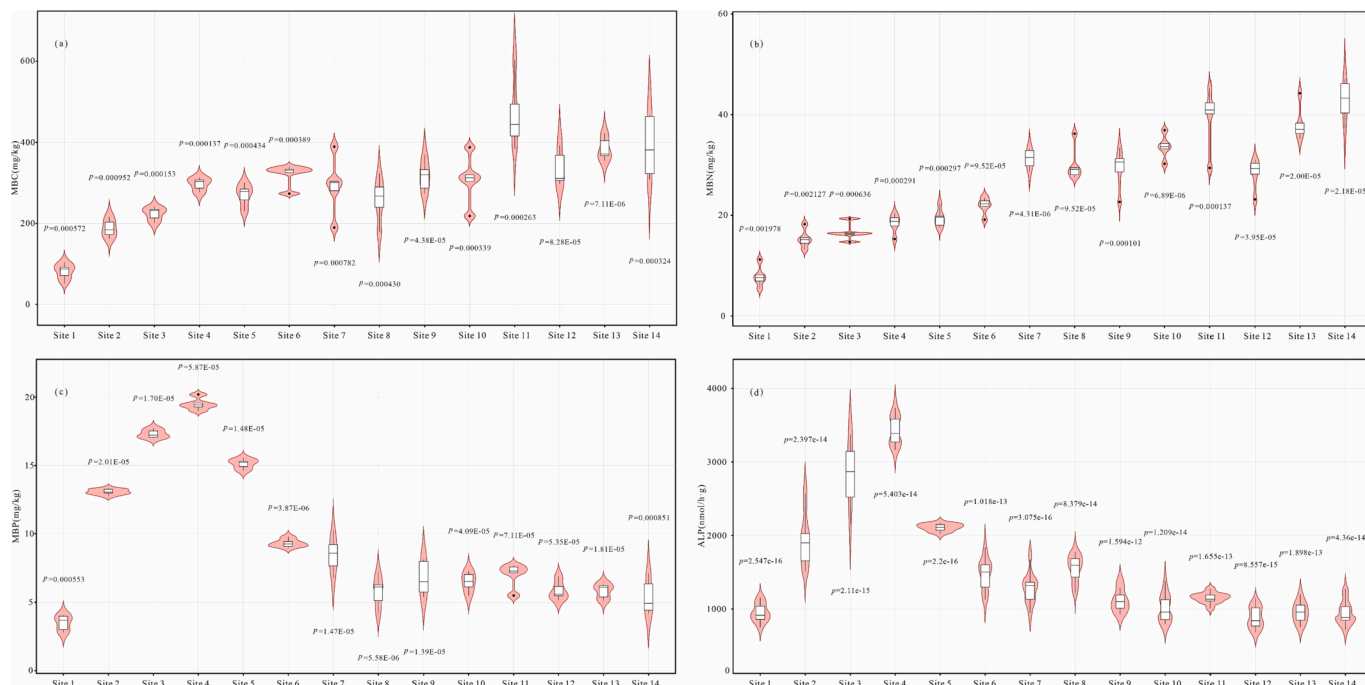


Fig. 3. Changes in soil alkaline phosphatase and microbiota C, N, P along the landslide chronosequence. In the box charts: the top of box is 75th percentile, the center of box is median, the bottom of box is 25th percentile, and the upper and lower ends of the vertical line are the maximum and minimum data values, respectively. In the violin chart: the width of the violin chart is the frequency.

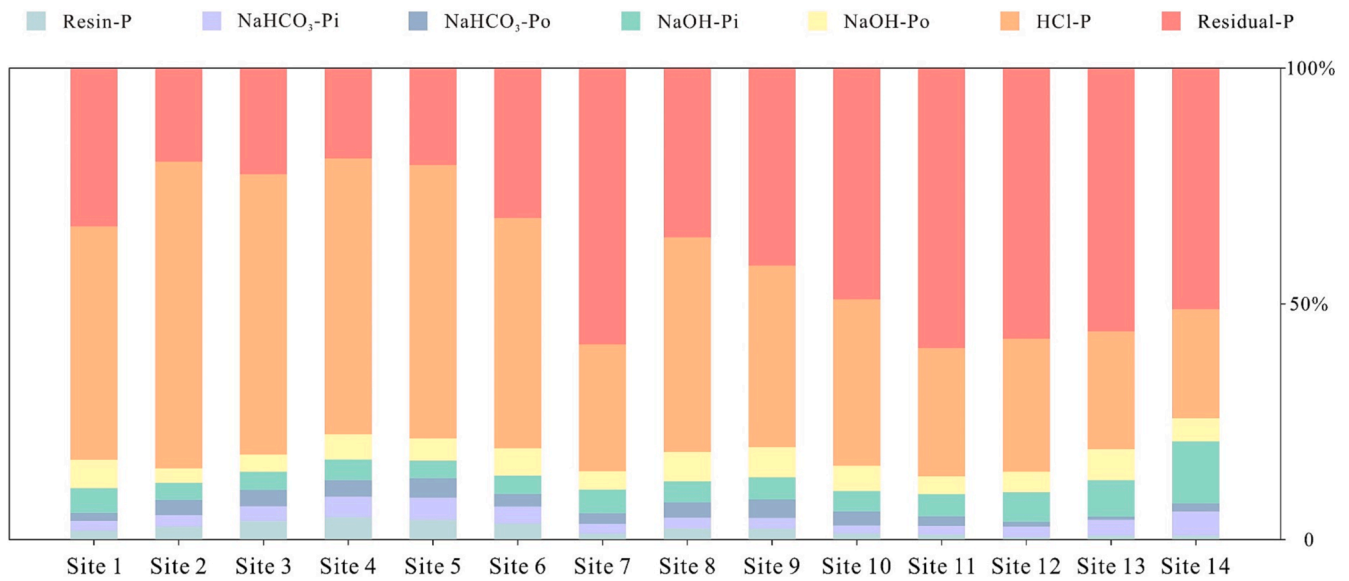


Fig. 4. Changes in soil phosphorus fractions along the landslide chronosequence. Resin-P: resin-extractable phosphorus; NaHCO₃-Pi: bicarbonate-extractable inorganic phosphorus; NaHCO₃-Po: bicarbonate-extractable organic phosphorus; NaOH-Pi: sodium hydroxide-extractable inorganic phosphorus; NaOH-Po: sodium hydroxide-extractable organic phosphorus; HCl-P: hydrochloric acid-extractable phosphorus.

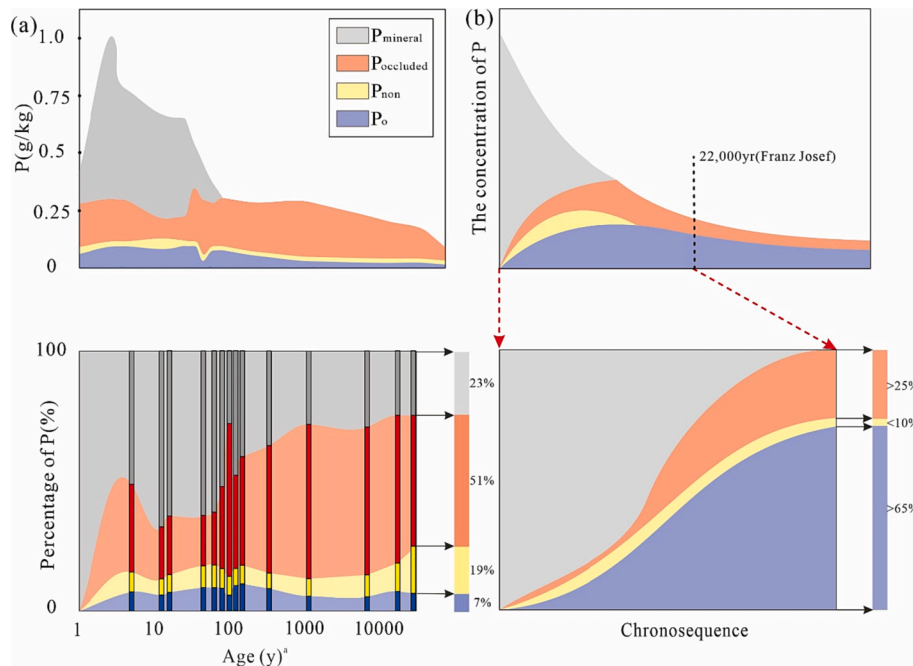


Fig. 5. Changes in the soil phosphorus pool. P-mineral: primary mineral phosphorus (HCl-P); P-occluded: occluded phosphorus (Residual-P); P-non: nonoccluded phosphorus (sum of NaHCO₃-Pi, NaOH-Pi); P-organic: organic phosphorus (sum of NaHCO₃-Po and NaOH-Po). The amount of P fraction is based on the area g/kg; and the percentage of P fraction over to total phosphorus (%). a: the chronosequence derived from landslides on the upper reach of Minjiang River, Western Sichuan, China; b: New Zealand chronosequence (Walker and Syers, 1976).

larger proportion of Pt in the soils. NaOH-Pi concentrations ranged from 10.94 to 42.41 mg/kg (3.55–8.37 % of Pt), while NaOH-Po concentrations ranged from 6.51 to 49.35 mg/kg (2.90–6.73 % of Pt) (Fig. 4). Among the P fractions, HCl-P represented the largest proportion in soils aged from 5 to 89 years. Its concentrations ranged from 324.51 to 774.76 mg/kg, accounting for 43.79–64.96 % of Pt. However, as soil development progressed, the concentrations of HCl-P declined rapidly. In soils aged from 89 to 1000 years, HCl-P concentrations ranged from 104.77 to 283.58 mg/kg, representing 27.16–45.38 % of Pt (Fig. 4). Further reduction in HCl-P concentrations (29.77–79.77 mg/kg,

accounting for 22.77–27.92 % of Pt) was observed in soils aged from 1000 to 22000 years. Lastly, the concentrations of Residual P, which encompassed the remaining P fractions, also showed a decreasing trend with soil age (90.58–385.76 mg/kg). However, the ratio of Residual P to Pt increased with soil age, ranging from 19.24 to 69.58 % (Fig. 4).

4. Discussion

4.1. Comparison with the Walker and Syers model

The Walker and Syers (1976) model emerged from a comprehensive investigation of chronosequences in humid and temperate regions of New Zealand. Its robustness has been demonstrated across diverse chronosequences encompassing different parent materials, climates, and vegetation types (Crews et al., 1995; Selmants and Hart, 2010). However, it should be noted that some studies have indicated its limited applicability in arid environments (Lajtha and Schlesinger, 1988) or tropical regions (Schlesinger et al., 1998). The fundamental premise of the Walker and Syers (1976) model is the progressive decline of primary mineral P during soil development. This decline occurs concurrently with the accumulation of organic and occluded P fractions. As soils undergo further maturation, the primary mineral P fraction becomes entirely exhausted, leading to the prevalence of organic and occluded P

within the residual P pool (Fig. 6b). The observed patterns in the concentrations of soil P fractions along the landslide chronosequence align with the anticipated trends outlined by the Walker and Syers (1976) model. As soil development progresses, there is a notable decline in the concentrations of all P fractions. This decline can be attributed to substantial P losses from the terrestrial ecosystem via surface runoff and leaching processes (Fig. 6a, b).

Nevertheless, the proportion of P fractions within the Pt exhibits notable variations along the landslide chronosequence, deviating significantly from the predictions of the Walker and Syers (1976) model (Fig. 6a), which supports our first hypothesis. According to Walker and Syers (1976), primary mineral P is expected to be rapidly depleted during soil development, resulting in a negligible proportion of primary mineral P in Pt at the late stages of soil development (Fig. 6b). While the declining proportion of primary mineral P aligns with the predictions of the Walker and Syers (1976) model, it is noteworthy that the proportion of primary mineral P in Pt reaches 23 % at the late stages of soil

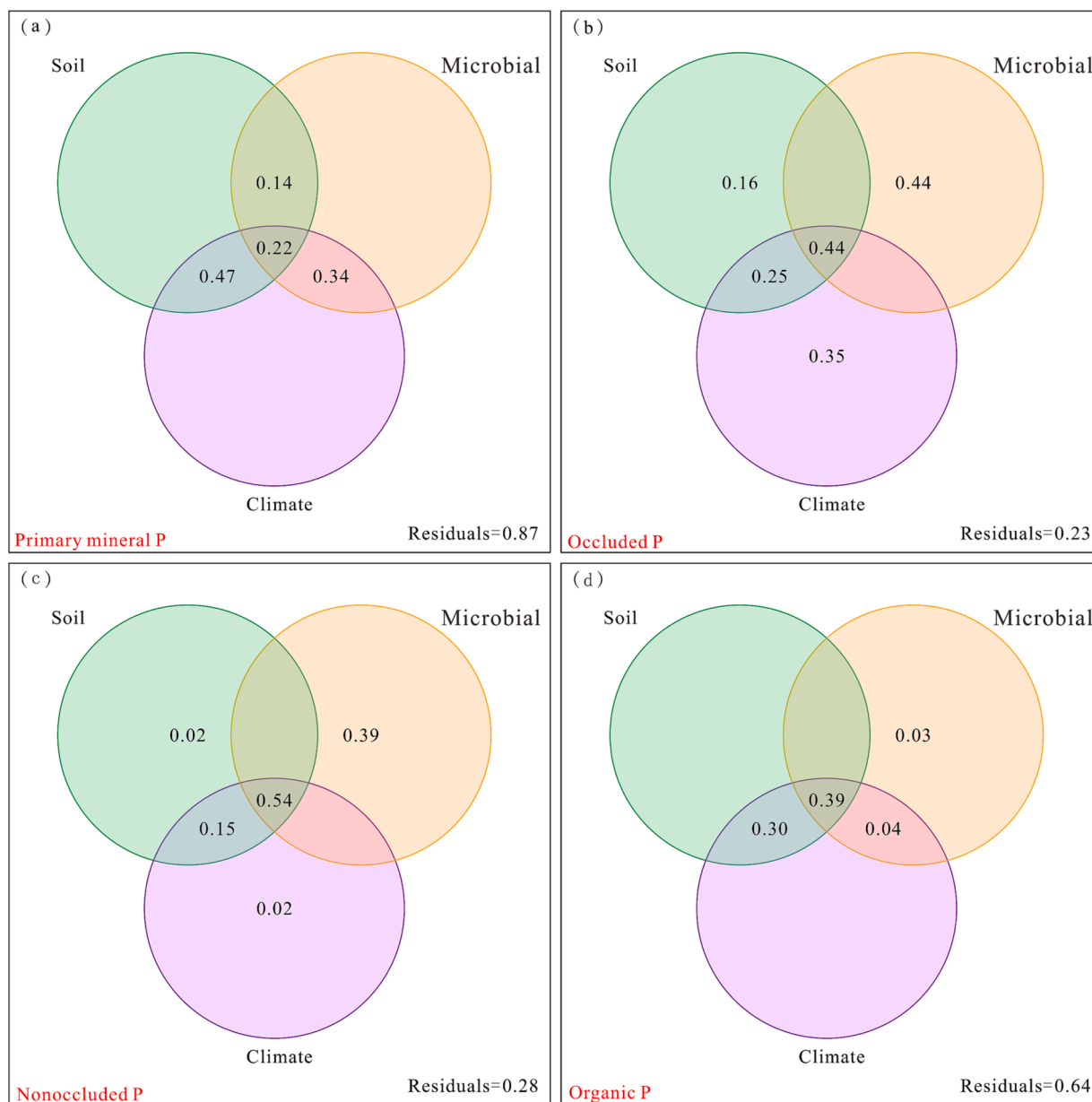


Fig. 6. Variation partitioning analysis showing the effects of environmental drivers (climate, microbes, and soil) on different fractions of phosphorus. Climate includes aridity index (AI), mean annual precipitation (MAP), mean annual temperature (MAT); Soil includes soil bulk density (BD), clay content of soil (clay), soil pH (pH), soil total C (TC), soil total N (TN), soil organic matter (SOM); Microbes includes soil microbiomes C, N, P (MBC, MCN, MBP), soil alkaline phosphatase (ALP).

development along the landslide chronosequence, despite the soil being over 22,000 years old (Fig. 6a). The observed phenomenon can be attributed to the landform characterized by frequent landslides within the study area. The presence of landslide landforms significantly increases the likelihood of soil erosion. This leads to the loss of soil P in terrestrial ecosystems, while simultaneously replenishing the primary mineral P within the soil (Eger et al., 2018). As a result, the proportion of primary mineral P within the Pt remains at 23 % even during the advanced stages of soil development. Contrary to the predictions put forth by the Walker and Syers (1976) model, our findings reveal that the Po did not assume dominance in the soil Pt at the late stages of soil development. Along the landslide chronosequence, even in the oldest soils (Site 14, soil age = 22,000 years), Po constituted a mere 7 % of the Pt (Fig. 6a). This value falls significantly below the predicted value (>65 %) of the Walker and Syers (1976) model (Fig. 6b). The observed dynamics can be attributed to the vegetation succession patterns within the study area. The substantial presence of Po at the early-stage soils of most soil chronosequences can be attributed to the rapid accumulation of soil organic matter during initial soil development phases. A pertinent example is provided by Celi et al. (2013), who documented the swift organic matter buildup resulting from Scots pine revegetation in a decommissioned sand quarry situated in Northwestern Russia. Remarkably, this accumulation occurred within a relatively cold environment, merely 40 years after pedogenesis initiation. However, in the study area, characterized by a distinct landform in the form of a landslide, the progression of vegetation succession was notably sluggish. Consequently, this prolonged progression significantly influenced the accumulation of Po.

In summary, along the landslide chronosequence, observed patterns soil P fraction concentrations align with the Walker and Syers (1976) model. However, the proportion of P fractions deviates from the model. Despite the soil being over 22,000 years old, primary mineral P remains at 23 % of the Pt due to frequent landslides replenishing the P stocks. And contrary to the model, organic P constitutes only 7 % even in the oldest soils, likely due to slow vegetation succession at landslide remains.

4.2. Effects of environmental factors (soil, climate, microbes) on soil phosphorus fractions

In our study, the effects of environmental factors, including soil properties, climate conditions, and microbial activities, on soil P fractions was examined. As depicted in Fig. 6a, our findings indicate that soil properties, climate conditions, and microbial activities did not exhibit a significant positive impact on the concentrations of primary mineral P. This conclusion is supported by the residuals value of 0.87, suggesting a limited explanatory power of environmental factors in relation to primary mineral P. This limited explanation is primarily attributed to the absence of rock weathering factors in Fig. 6a. That primary mineral P in the soil originates primarily from the weathering of rocks and subsequent transformation or conversion into other P fractions as effects by environmental factors (Turner and Haygarth, 2001). Consequently, the sole positive contribution to the primary mineral P fraction stems from rock weathering. The absence of this crucial factor in Fig. 6a. Environmental factors exhibit a notable positive effect on the concentration of occluded P, as evidenced by Fig. 6b (residuals = 0.23). This phenomenon can be attributed to the ongoing conversion of primary mineral P into occluded P and nonoccluded P throughout the soil formation process (Turner and Haygarth, 2001). Occluded P, characterized by its limited availability to plants and microorganisms (Condon et al., 1990), accumulates persistently during soil development (Fig. 7a). Therefore, the environmental factors collectively exert significant positive contributions to the accumulation of occluded P. Microbial activity exerted a substantial positive impact on the concentration of nonoccluded P, as demonstrated in Fig. 7c (residuals = 0.28). During the early stages of soil development, the rise in nonoccluded P primarily stems from the presence of primary mineral P (Turner and Haygarth, 2001). Nonoccluded P, characterized by its high bioavailability to plants and microorganisms, gradually declines in concentration with soil age (Richardson and Simpson, 2011). When the concentration of nonoccluded P becomes insufficient to meet the demands of plants and microorganisms, microorganisms possess the capability to convert a portion of Po into non-occluded P (Fig. 7a) (Vitousek et al., 1997). Environmental factors exhibit a relatively limited explanations for Po, as indicated by Fig. 6d

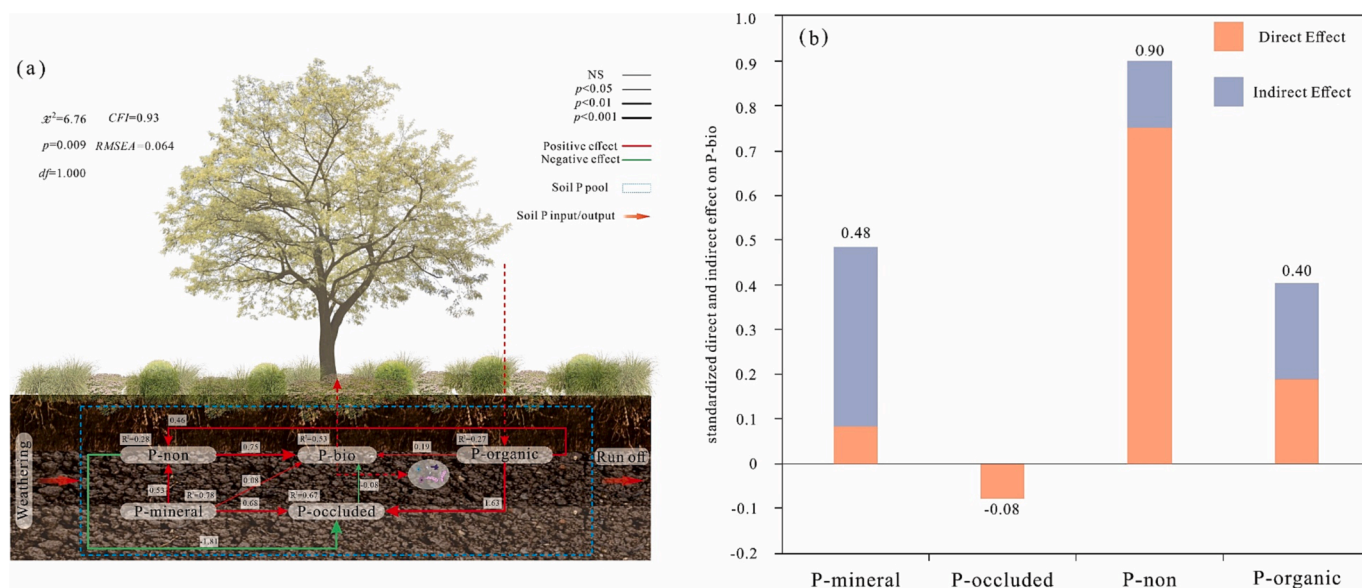


Fig. 7. Evaluation of predictor variables for soil bioactive phosphorus using structural equation modeling. P-mineral: primary mineral phosphorus (HCl-P); P-occluded: occluded phosphorus (Residual-P); P-non: nonoccluded phosphorus (NaCHO₃-Pi, NaOH-Pi); P-organic: organic phosphorus (NaHCO₃-Po and NaOH-Po); P-bio: bioactive phosphorus (Resin-P).a: Significance of line thickness response; Positive and negative effects were expressed as different colors of the arrow (red: positive effect; green: negative effect); Numbers on each arrow and column indicate the standardized path coefficients and standardized total effect, respectively; R² near each endogenous variable means the explanation power of variance; b: Blue and orange arrows indicate positive and negative flows of causality, respectively; Numbers on the arrow indicate significant standardized path coefficients.

(residuals = 0.64). This can be attributed to the predominant source of Po in the soil, which is primarily derived from plant-derived organic matter (Turner and Haygarth, 2001b). Plants play a crucial role in influencing the availability and cycling of bioavailable phosphorus in ecosystems. Through various mechanisms, plants can acquire, utilize, and release P, thereby shaping the dynamics of this essential nutrient. Firstly, plants have evolved adaptations to enhance bioavailable phosphorus acquisition from the soil. They develop an extensive root system with root hairs and mycorrhizal associations to increase the surface area for nutrient absorption. Additionally, plants can release organic acids, enzymes, and phosphatase enzymes into the rhizosphere, facilitating the mobilization and solubilization of organic and inorganic forms of P in the soil, contributing to the conversion of bioavailable phosphorus (Richardson and Simpson, 2011). Furthermore, plants can influence the cycling of P through litterfall and root turnover. When plant tissues senesce and fall to the ground, they contribute to the input of organic matter and associated P into the soil. Decomposition of plant residues by soil microorganisms' releases P, making it available for uptake by plants and other organisms. Similarly, when roots die and decompose, they release P back into the soil, contributing to the overall P cycling (Turner and Haygarth, 2001). However, since the effects of vegetation factors is not explicitly captured in Fig. 6d, it becomes challenging to fully elucidate the variations observed in Po concentrations solely based on the examined environmental factors.

Overall, environmental factors had a limited effect on the concentration of primary mineral P but exhibited a notable positive effect on occluded P and nonoccluded P. Microbial activity played a significant role in nonoccluded P concentration, while changes in Po concentrations were not fully explained by the examined environmental factors due to the contribution of plant litter decomposition.

4.3. The supply of soil bioavailable phosphorus along the landslide chronosequence

The release of soil available P from other P fractions controlled by many physical, chemical and biological processes such as sorption/desorption, precipitation/dissolution, mineralization and weathering (Lambers et al., 2008; Vitousek et al., 2010; Barrow, 2015). The outcomes derived from the utilization of structural equation modeling (SEM) revealed noteworthy correlations between nonoccluded P, primary mineral phosphorus P, and Po with changes in P-bio. Nonoccluded P exerted a direct regulatory effect on the concentration of P-bio, while primary mineral P and Po primarily effected P-bio through indirect pathways (Fig. 7b). And Po exhibited a weak positive direct effect on P-bio, whereas occluded P displayed a negative correlation with P-bio (Fig. 7b). These findings indicate that nonoccluded P serves as the primary source of soil P-bio, with primary mineral P exerting its regulatory effects indirectly via nonoccluded P. Organic P does not seem to play a significant role in contributing to P-bio, that is contrary to our hypothesis. We attribute this observation is due to high levels of primary mineral P present in the soil along the landslide chronosequence. Typically, during the early stages of soil development, a substantial portion of primary mineral P transformation into nonoccluded P and occluded P. Nonoccluded P acts as a crucial supplier of P-bio for plants and microorganisms. However, as soil development progresses, the reserves of primary mineral P become depleted, resulting in a reduction of the major source of nonoccluded P and subsequently impacting the quantity of P-bio (Vitousek and Howarth, 1991). Consequently, microorganisms initiate the conversion of a portion of Po into nonoccluded P and P-bio to meet the demands of plants and microorganisms (Turner and Haygarth, 2001), gradually establishing Po as the primary source of P-bio. However, the distinctive landform conditions (landslides) prevalent in the study area facilitate the continuous replenishment of primary mineral P during the soil development (Fig. 1, Fig. 4, Fig. 5). As a result, primary mineral P consistently supplies nonoccluded P to the soil, thereby establishing nonoccluded P as the principal source of P-bio

along the landslide chronosequence (Fig. 7).

Sum up, nonoccluded P emerges as the primary contributor to P-bio in soil, whereas Po exhibits limited effect on P-bio. This observation can be attributed to the distinctive landform conditions, specifically the presence of landslides, within the study area, which sustain elevated levels of primary mineral P throughout soil development. Consequently, the continuous availability of nonoccluded P guarantees a reliable supply of P-bio.

5. Conclusion

Based on our research of the long-term dynamic of soil P fractions along a landslide chronosequence. We have discerned notable patterns. The inherent instability of landslide landforms has been found to foster the enhanced liberation of primary mineral P, resulting in the primary mineral P in soil being one of the principal components of soil Pt during soil development. Simultaneously, the decelerated progression of vegetation succession on landslide landforms hampers the accumulation of Po during the process of soil formation. Furthermore, our investigation has unveiled that environmental factors exhibit a notable positive influence on the buildup of occluded P and nonoccluded P, indicating the transformation of primary mineral phosphorus into these specific fractions during pedogenesis. Nevertheless, it is noteworthy that the observed changes in Po concentrations cannot be comprehensively elucidated by the examined environmental factors alone, as the primary source of Po in the soil is attributed to the decomposition of plant litter. Furthermore, our findings indicate that soil P-bio predominantly originates from nonoccluded P rather than Po. This observation can be attributed to the substantial abundance of primary mineral P and the ongoing conversion of primary mineral P to nonoccluded P, thereby positioning nonoccluded P as the principal source of P-bio. Considering these results, our study underscores the significance of landslide chronosequences as exemplars of long-term ecosystem development under unstable landforms. This research represents a modification of the classic Walker and Syers model of P transformations during pedogenesis. However, there are some limitations of this study that need to be noted. Firstly, this study only analyzed soil samples from a specific geographic area and therefore the applicability of the results may be limited by geographic location. Further studies should consider replication and validation in different geographical areas and soil types. Secondly, the sample size of this study was relatively small, which may affect the representativeness and statistical significance of the results. A larger sample size could provide more convincing evidence and increase the reliability of the findings. Finally, the complexity of unstable landscapes also affects the accuracy of the landslide soil chronosequence, and in the future, we need to utilize more soil age determination methods to ensure that the age of soils is clarified. In conclusion, despite some important findings in this study, more research is needed to overcome the above limitations and to explore the complexity and diversity of soil development processes in further depth.

Declaration of Competing Interest

The authors declare that they have no known competing financial interests or personal relationships that could have appeared to influence the work reported in this paper.

Data availability

Data will be made available on request.

Acknowledgments

The research reported in this manuscript is funded by the Key Research and Development Projects Foundation of Sichuan, China (2018JZ0075), the National Natural Science Foundation of China

(42271064).

References

- Adil, N., Atiq, A.R., Saleemul, H., Youba, S., 2003. Integrating sustainable development into the Fourth Assessment Report of the Intergovernmental Panel on Climate Change. *Clim. Pol.* 3 (1), S9–S17.
- An, W.P., Zhao, J.Q., Yan, X.B., 2008. Tectonic deformation of lacustrine sediments in Qiangyang on the Minjiang fault zone and ancient earthquake. *Seismol. Geol.* 30 (4), 980–988. In Chinese.
- Barrow, N.J., 2015. A mechanistic model for describing the sorption and desorption of phosphate by soil. *Eur. J. Soil Sci.* 66 (1), 9–18.
- Bogaart, P., Zee, S.E., 2010. Coupled hydrological and biogeochemical modeling of hillslope processes: implications for phosphorus dynamics. *J. Geophys. Res. Biogeo.* 115 (G3).
- Brookes, P.C., Powlson, D.S., Jenkinson, D.S., 1982. Measurement of microbial biomass phosphorus in soil. *Soil Biol Biochem.* 14 (4), 319–329.
- Blonska, E., Lasota, J., Piaszczyk, W., Wiecheć, M., Anna, K.I., 2018. The effect of landslide on soil organic carbon stock and biochemical properties of soil. *J. Soils Sediments.* 18 (8), 2727–2737.
- Celi, L., Cerli, C., Turner, B.L., Santoni, S., Bonifacio, E., 2013. Biogeochemical cycling of soil Phosphorus during natural revegetation of Pinussylvestris on disused sandquarries in Northwestern Russia. *Plant Soil.* 367, 121–134.
- Chai, H.J., Liu, H.C., Zhang, Z.Y., 1995. The catalog of Chinese landslide dam events. *J. Hazard Mater.* 4, 1–9. In Chinese.
- Chen, Y.L., Ding, J.Z., Peng, Y.F., Li, F., Yang, G.B., Liu, L., Qin, S.Q., Fang, K., Yang, Y.H., 2016. Patterns and drivers of soil microbial communities in Tibetan alpine and global terrestrial ecosystems. *J. Biogeogr.* 43 (10), 2027–2039.
- Chen, Z.X., Yang, S.L., Luo, Y.L., Chen, H., Liu, L., Liu, X.J., Wang, S.Y., Yang, J.H., Tian, W.D., Xia, D.S., 2022. Hirm variation in the ganzhi loess of the eastern tibetan plateau since the last interglacial period and its paleotemperature implications for The Source Region. *Gondw. Res.* 101, 233–242.
- Condron, L.M., Goh, K.M., Newman, R.H., Tiessen, H., 1990. The role of phosphorus in the transformation of apatite in soils: An evaluation of the evidence. *Geoderma* 46 (1–3), 145–168.
- Crews, T.E., Kitayama, K., Fownes, J.H., Riley, R., Herbert, D., Dieter, M.D., Vitousek, P. M., 1995. Changes in soil phosphorus fractions and ecosystem dynamics across a long chronosequence in Hawaii. *Ecology* 76 (5), 1407–1424.
- Cruden, D., Varnes, D.J., 1996. Landslide types and processes. In: Turner, A.K., Schuster, R.L. (Eds.), *Landslides: Investigation and Mitigation*, 247. National Academy Press, Washington, D.C., pp. 36–75.
- Cruden, D.M., 1991. A simple definition of a landslide. *Bull. Int. Assoc. Eng. Geol.* 43 (1), 27–29.
- Cui, Y.X., Bing, H.J., Daryl, L.M., Manuel, D.B., Ye, L., Yu, J.L., Zhang, S.P., Wang, X., Peng, S.S., Guo, X., Zhu, B., Chen, J., Tan, W.F., Wang, Y.Q., Zhang, X.C., Fang, L.C., 2022. Eoenzymatic stoichiometry reveals widespread soil phosphorus limitation to microbial metabolism across Chinese forests. *Commun. Earth Environ.* 3 (1).
- Delgado-Baquerizo, M., Maestre, F.T., Gallardo, A., Bowker, M.A., Wallenstein, M.D., Quero, J.L., Ochoa, V., Gozalo, B., García-Gómez, M., Soliveres, S., García-Palacios, P., Berdugo, M., Valencia, E., Escobar, C., Arredondo, T., Barraza-Zepeda, C., Bran, D., Carreira, J.A., Chaiieb, M., Conceicao, A.A., Derak, M., Eldridge, D.J., Escudero, A., Espinosa, C.L., Gaitan, J., Gatica, M.G., Gomez-Gonzalez, S., Guzman, E., Gutierrez, J.R., Florentino, A., Hepper, E., Hernandez, R. M., Huber-Sannwald, E., Jankju, M., Liu, J., Mau, R.L., Miriri, M., Moneris, J., Naseri, K., Nouni, Z., Polo, V., Prina, A., Pucheta, E., Ramirez, E., Ramirez-Collantes, D.A., Romao, R., Tighe, M., Torres, D., Torres-Díaz, C., Ungar, E.D., Val, J., Wamiti, W., Wang, D., Zaady, E., 2013. Decoupling of soil nutrient cycles as a function of aridity in global drylands. *Nature* 502 (7473), 672–676.
- Eger, A., Kyungsoo, Y., Peter, C.A., Gustavo, B., Larsen, I.J., Condron, L.M., Wang, X., Simon, M.M., 2018. Does soil erosion rejuvenate the soil phosphorus inventory. *Geoderma* 332, 45–55.
- Evans, S., Clague, J.J., 1994. Recent climatic change and catastrophic geomorphic processes in mountain environments. *Geomorphology* 10 (1), 107–128.
- Fang, X.M., Lu, L.Q., Mason, J.A., Yang, S.L., An, Z.S., Li, J.J., Guo, Z.L., 2003. Pedogenic response to millennial summer monsoon enhancements on the Tibetan Plateau. *Quat. Int.* 106, 79–88.
- Fang, X.M., 1994. The origin and provenance of Malan loess from the eastern edge of Tibetan plateau and its adjacent areas. *Sci. China Ser. B-Chem.* 24 (5), 539–546. In Chinese.
- Gan, J.J., Han, W., Chun, T., Huang, C., Chen, J., 2015. Mechanism and characteristics of multiple catastrophic mudslides of tasi ditch in Li county of Sichuan Province. *J. Catastrophol.* 30 (4), 59–63. In Chinese.
- Geertsema, M., Clague, J.J., Schwab, J.W., Evans, S.G., 2006. An overview of recent large catastrophic landslides in northern British Columbia, Canada. *Eng. Geol.* 83 (1), 120–143.
- German, D.P., Weintraub, M.N., Grandy, A.S., Lauber, C.L., Rinke, Z.L., Allison, S.D., 2011. Optimization of hydrolytic and oxidative enzyme methods for ecosystem studies. *Soil Biol. Biochem.* 43 (7), 1387–1397.
- Han, Y., Huh, Y., Derry, L., 2015. Ge/Si ratios indicating hydrothermal and sulfide weathering input to rivers of the Eastern Tibetan Plateau and Mt Baekdu. *Chem. Geol.* 410, 40–52.
- He, J.B., Wu, Y.H., Bing, H.J., Zhou, J., Zhu, H., 2023. Soil chronosequence derived from landslides on the upper reach of Minjiang River, western China. *J. Mt. Sci.* 20 (5), 1282–1292.
- Hedley, M.J., Stewart, J.W.B., 1982. Method to measure microbial phosphate in soils. *Soil Biol. Biochem.* 14 (4), 377–385.
- Hemingway, J.D., Hilton, R.G., Hovius, N., Eglinton, T.I., Haghpor, N., Wacker, L., Chen, M.C., Galy, V.V., 2018. Microbial oxidation of lithospheric organic carbon in rapidly eroding tropical mountain soils. *Science* 360 (6385), 209–212.
- Hilton, R.G., Galy, A., Hovius, N., 2008. Riverine particulate organic carbon from an active mountain belt: Importance of landslides. *Glob. Biogeochem. Cycles.* 22 (1).
- Hilton, R.G., Meunier, P., Hovius, N., Bellingham, P.J., Galy, A., 2011. Landslide impact on organic carbon cycling in a temperate montane forest. *Earth Surf. Process Landf.* 36 (12), 1670–1679.
- Hou, E., Wen, D., Kuang, Y., Cong, J., Chen, C., He, X., Heenan, M., Lu, H., Zhang, Y., 2018. Soil pH predominantly controls the forms of organic phosphorus in topsoils under natural broadleaved forests along a 2500 km latitudinal gradient. *Geoderma* 315, 65–74.
- Korup, O., 2004. Geomorphic implications of fault zone weakening: Slope instability along the Alpine Fault, South Westland to Fiordland. *N Z J Geol. Geophys.* 47 (2), 257–267.
- Kouno, K., Tuchiya, Y., Ando, T., 1995. Measurement of soil microbial biomass phosphorus by an anion-exchange membrane method. *Soil Biol. Biochem.* 27 (10), 1353–1357.
- Lajtha, K., Schlesinger, W.H., 1988. The biogeochemistry of phosphorus cycling and phosphorus availability along a desert soil chronosequence. *Ecology* 69, 24–39.
- Lambers, H., Raven, J., Shaver, G., Smith, S., 2008. Plant nutrient-acquisition strategies change with soil age. *Trends Ecol. Evol.* 23 (2), 95–103.
- Lu, H.H., Yi, G.H., Zhang, T.B., Li, J.J., Wang, G.Y., Qin, Y.B., Wen, B., 2021. Variations in vegetation cue with climate change and human activity during growing seasons in the Western Sichuan Plateau, China. *Remote Sens. Lett.* 12 (5), 419–428.
- McLennan, S.M., 1993. Weathering and global denudation. *J. Geol.* 101 (2), 295–303.
- Nesbitt, H.W., Young, G.M., 1982. Early proterozoic climate and plate motions inferred from major element chemistry of lites. *Nature* 299 (5885), 715–717.
- Nie, G.Z., Gao, J.G., Deng, Y., 2004. Preliminary study on earthquake-induced dammed lake. *Quart. Sci.* 24 (3), 293–301. In Chinese.
- Parker, R.N., Densmore, A.L., Rosser, N.J., Michele, M., Li, Y., Huang, R., Whadcoat, S., Petley, D.N., 2011. Mass wasting triggered by the 2008 Wenchuan earthquake is greater than orogenic growth. *Nat. Geosci.* 4 (7), 449–452.
- Petley, D., 2012. Global patterns of loss of life from landslides. *Geology* 40 (10), 927–930.
- Poeplau, C., Don, A., Vesterdal, L., Leifeld, J., Wesemael, B.S., Schumacher, J., Gensior, A., 2011. Temporal dynamics of soil organic carbon after land-use change in the temperate zone e carbon response functions as a model approach. *Glob. Change Biol.* 17 (7), 2415–2427.
- Richardson, A.E., Simpson, R.J., 2011. Soil microorganisms mediating phosphorus availability. *Plant Physiol.* 156 (3), 989–996.
- Schlesinger, W.H., Bruijnzel, L.A., Bush, M.B., Klein, E.M., Mace, K.A., Raikes, J.A., Whittaker, R.J., 1998. The biogeochemistry of phosphorus after the first century of soil development on Rakata Island, Krakata, Indonesia. *Biogeochemistry.* 40, 37–55.
- Schmidt, S.K., Reed, S.C., Nemerugut, D.R., Grandy, A.S., Cleveland, C.C., Weintraub, M. N., Hill, A.W., Costello, E.K., Meyer, A.F., Nef, J.C., Am, M., 2008. The earliest stages of ecosystem succession in high-elevation (5000 metres above sea level), recently deglaciated soils. *Proc R Soc B Biol Sci.* 275 (1653), 2793–2802.
- Schulz, S., Brankatschk, R., Dümig, A., Kögel-Knabner, I., Schloter, M., Zeyer, J., 2013. The role of microorganisms at different stages of ecosystem development for soil formation. *Biogeochemistry* 10 (6), 3983–3996.
- Selmants, P.C., Hart, S.C., 2010. Phosphorus and soil development: does the walker and syers model apply to semiarid ecosystems? *Ecology* 91 (2), 474–484.
- Tate, K.R., Scott, N.A., Parshotam, A., Brown, L., Wilde, R.H., Giltrap, D.J., Trustrum, N. A., Gomez, B., Ross, D.J., 2000. A multi-scale analysis of a terrestrial carbon budget: Is New Zealand a source or sink of carbon? *Agric. Ecosyst Environ.* 82 (1), 229–246.
- Tian, H.Q., Wang, S.Q., Liu, J.Y., Pan, S.F., Chen, H., Zhang, C., Shi, X.Z., 2006. Patterns of soil nitrogen storage in China. *Global Biogeochem. Cycles* 20 (1), GB1001.
- Tiessen, H., Moir, J.O., 1993. Characterization of available P by sequential extraction. In: Carter, M.R. (Ed.), *Soil Sampling and Methods of Analysis*. Lewis Publishers, Boca Raton, Ann Arbor, London, pp. 75–85.
- Turner, B.L., Haygarth, P.M., 2001. Phosphorus forms and concentrations in leachate from soils of differing pedology, land use and management. *J. Environ. Qual.* 30 (2), 508–520.
- Vindusková, O., Pánek, T., Frouz, J., 2019. Soil C, N and P dynamics along a 13 ka chronosequence of landslides under semi-natural temperate forest. *Quat Sci Rev.* 213C, 18–29.
- Vitousek, P.M., Howarth, R.W., 1991. Nitrogen limitation on land and in the sea: How can it occur? *Biogeochemistry* 13 (2), 87–115.
- Vitousek, P.M., Porder, S., Houlton, B.Z., Chadwick, O.A., 2010. Terrestrial phosphorus limitation: mechanisms, implications, and nitrogen–phosphorus interactions. *Ecol Appl.* 20 (1), 5–15.
- Walker, T.W., Syers, J.K., 1976. The fate of phosphorus during pedogenesis. *Geoderma* 15 (1), 1–19.
- Walker, L.R., Velázquez, E., Shiels, A.B., 2009. Applying lessons from ecological succession to the restoration of landslides. *Plant Soil.* 324 (1), 157–168.
- Walker, L.R., Wardle, D.A., Bardgett, R.D., Clarkson, B.D., 2010. The use of chronosequences in studies of ecological succession and soil development. *J. Ecol.* 98 (4), 725–736.
- Wang, L.S., Wang, X.Q., Xu, X.N., Cui, J., 2007. What happened on the upstream of Minjiang River in Sichuan Province 20000 years ago? *Earth Sci. Front.* 14 (4), 189–196. In Chinese.

- Wang, Z., Li, X., Li, Y., Zhang, X., 2021. Assessing the impacts of land use change on ecosystem services in the western Sichuan Plateau, China. *Land* 10 (2), 198.
- Wardle, D.A., Lawrence, R.W., Bardgett, R.D., 2004. Ecosystem properties and forest decline in contrasting long-term chronosequences. *Science* 308 (5772), 633c.
- Watanabe, M.D.B., Ortega, E., 2011. Ecosystem services and biogeochemical cycles on a global scale: valuation of water, carbon and nitrogen processes. *Environ. Sci. Policy* 14 (6), 594–604.
- Westheimer, F.H., 1987. Why nature chose phosphates. *Science* 235 (4793), 1173–1178.
- Wilkinson, D.M., 2008. Testate amoebae and nutrient cycling: Peering into the black box of soil ecology. *Trends Ecol Evol.* 23, 596–599.
- Wu, Y.H., Zhou, J., Bing, H.J., Sun, H.Y., Wang, J.P., 2015. Rapid loss of phosphorus during early pedogenesis along a glacier retreat chronosequence, Gongga Mountain (Sw China). *PeerJ* 3 (1–2), 26557441.
- Xie, H., Zhong, D.L., Li, Y., Wei, F.Q., 2004. Features of debris flows in the upper reaches of the Changjiang River. *Resources and Environment in the Yangtze Basin.* 13 (1), 94–99. In Chinese.
- Xu, Q., Li, W.L., Dong, X.J., Xiao, X.X., Fan, X.M., Pei, X.J., 2017. The Xinmocun landslide on June 24, 2017 in Maoxian, Sichuan: characteristics and failure mechanism. *Chin. J. Rock Mech. Eng.* 36 (11), 2612–2628. In Chinese.
- Yang, L., Luo, P., Wen, L., Li, D., J., 2016. Soil organic carbon accumulation during post-agricultural succession in a karst area. Southwest China. *Sci Rep* 6 (1), 37118.
- Zhong, J., Li, S., Li, Z., Zhu, X.T., Yi, Y.B., Ma, T.T., Xu, S., Liu, C.Q., 2022. Metamorphic fluxes of water and carbon in rivers of the Eastern Qinghai-Tibetan Plateau. *Sci. China Earth Sci.* 65 (4), 652–661.
- Zorner, R.J., Trabucco, A., Bossio, D.A., Verchot, L.V., 2008. Climate change mitigation: A spatial analysis of global land suitability for clean development mechanism afforestation and reforestation. *Agric. Ecosyst. Environ.* 126 (1–2), 67–80.